

# High-Mobility Aligned Pentacene Films Grown by Zone-Casting

Claudia M. Duffy,<sup>†</sup> Jens W. Andreasen,<sup>‡</sup> Dag W. Breiby,<sup>§</sup> Martin M. Nielsen,<sup>||</sup>  
Masahiko Ando,<sup>⊥</sup> Takashi Minakata,<sup>#</sup> and Henning Sirringhaus<sup>\*†</sup>

*Optoelectronics Group, Cavendish Laboratory, University of Cambridge, J.J. Thomson Avenue, Cambridge CB3 0HE, United Kingdom, Polymers for Energy Technology, Risø National Laboratory for Sustainable Energy, Technical University of Denmark, Frederiksborgvej 399, DK-4000 Roskilde, Denmark, Department of Physics, Norwegian University of Science and Technology, 7491 Trondheim, Norway, Centre for Molecular Movies, Niels Bohr Institute, University of Copenhagen, Universitetsparken 5, DK-2100 Copenhagen, Denmark, Hitachi Cambridge Laboratory, J.J. Thomson Avenue, Cambridge CB3 0HE, United Kingdom, and R&D Centre, Asahi-KASEI Corporation, 2-1 Samejima, Fuji-shi, Shizuoka-ken, Japan*

Received June 21, 2008. Revised Manuscript Received August 8, 2008

We investigate the growth and field-effect transistor performance of aligned pentacene thin films deposited by *zone-casting* from a solution of unsubstituted pentacene molecules in a chlorinated solvent. Polarized optical microscopy shows that solution processed pentacene films grow as large crystalline domains with pronounced anisotropy in the substrate plane, in contrast to vacuum sublimed pentacene films, which consist of small crystalline grains with random in-plane orientation. The high structural alignment is confirmed by in-plane and out-of-plane X-ray diffraction analysis, with out-of-plane  $00n$  reflections up to at least the seventh order, and a pronounced in-plane anisotropy with the  $a$ -axis of the triclinic unit cell predominantly aligned parallel to the zone-casting direction and the  $ab$ -plane parallel to the substrate. The average charge carrier mobility of the zone-cast pentacene devices depends strongly on the underlying dielectric. Divinylsiloxane-bis-benzocyclobutene (BCB) resin is found to be a suitable gate dielectric allowing reproducible film deposition and high field-effect mobilities up to  $0.4\text{--}0.7\text{ cm}^2/(\text{V s})$  and on/off ratios of  $10^6\text{--}10^7$ . A small mobility anisotropy is observed for devices with channels aligned along and perpendicular to the zone-casting direction.

## Introduction

Pentacene (PEN) is one of the most studied small molecule organic semiconductors as it exhibits some of the highest mobilities and on/off ratios among the p-type organic field-effect transistors.<sup>1</sup> The vast majority of these studies were conducted on polycrystalline films grown by vapor deposition.<sup>2,3</sup> The performance of vacuum sublimed PEN thin-film transistors (TFTs) depends strongly on the grain size<sup>4,5</sup> and texture<sup>6,7</sup> of the polycrystalline films. Recently, it has been shown by Minakata et al.<sup>8</sup> that unsubstituted PEN can be deposited from solution at elevated temperatures. From a

technological and commercial perspective, solution processing is attractive for low-cost, large-area TFT manufacturing. From the device physics perspective, solution-processed PEN allows a better understanding of the effect of film morphology and grain boundaries on device performance and stability. Grain sizes in vacuum-deposited films of PEN are relatively small, and grain boundaries have recently been shown to act as trapping centers for the accumulated charge carriers.<sup>9</sup> In contrast, large crystals are formed in the solution-processed PEN films, with an apparent reduction of the number of grain boundaries compared to vacuum sublimed PEN films.

Preferential orientation of organic molecules in the plane of the film has been demonstrated previously by mechanical alignment methods, such as rubbing,<sup>10</sup> friction transfer<sup>11</sup> or transfer printing,<sup>12</sup> as well as photoalignment methods.<sup>13</sup> Some acenes, such as anthracene and substituted pentacene, have been aligned from solution by drop-casting onto a tilted

\* Corresponding author. E-mail: hs220@cam.ac.uk.

<sup>†</sup> University of Cambridge.

<sup>‡</sup> Technical University of Denmark.

<sup>§</sup> Norwegian University of Science and Technology.

<sup>||</sup> University of Copenhagen.

<sup>⊥</sup> Hitachi Cambridge Laboratory.

<sup>#</sup> Asahi-KASEI Corporation.

- (1) Gundlach, D. J.; Lin, Y. Y.; Jackson, T. N.; Nelson, S. F.; Schlom, D. G. *IEEE Electron Device Lett.* **1997**, *18*, 87.
- (2) Ruiz, R.; Papadimitratos, A.; Mayer, A. C.; Malliaras, G. G. *Adv. Mater.* **2005**, *17*, 1795.
- (3) Schroeder, R.; Majewski, L. A.; Grell, M. *Appl. Phys. Lett.* **2003**, *83*, 3201.
- (4) Knipp, D.; Street, R. A.; Voelkel, A.; Ho, J. *J. Appl. Phys.* **2003**, *93*, 347.
- (5) Laquindanum, J. G.; Katz, H. E.; Lovinger, A. J.; Dodabalapur, A. *Adv. Chem. Mater.* **1996**, *8*, 2542.
- (6) Chou, W.-Y.; Cheng, H.-L. *Adv. Funct. Mater.* **2004**, *14*, 811.
- (7) Jin, S.-H.; Seo, H.-U.; Nam, D.-H.; Shin, W. S.; Choi, J.-H.; Yoon, U. C.; Lee, J.-W.; Song, J.-G.; Shin, D.-M.; Gal, Y.-S. *J. Mater. Chem.* **2005**, *15*, 5029.
- (8) Minakata, T.; Natsume, Y. *Synth. Met.* **2005**, *153*, 1.

- (9) Tello, M.; Chiesa, M.; Duffy, C. M.; Sirringhaus, H. *Adv. Funct. Mater.*, submitted.
- (10) Swiggers, M. L.; Xia, G.; Slinker, J. D.; Gorodetsky, A. A.; Malliaras, G. G.; Headrick, R. L.; Weslowski, B. T.; Shashidhar, R. N.; Dulcey, C. S. *Appl. Phys. Lett.* **2001**, *79*, 1300.
- (11) Kihara, H.; Ueda, Y.; Unno, A.; Hirai, T. *Mol. Cryst. Liq. Cryst.* **2004**, *424*, 195.
- (12) Kim, H.-H.; Bong, K.-W.; Lee, H. H. *Appl. Phys. Lett.* **2007**, *90*, 093505.
- (13) Guo, D.; Sakamoto, K.; Miki, K.; Ikeda, S.; Saiki, K. *Appl. Phys. Lett.* **2007**, *90*, 102117.

substrate,<sup>14</sup> dip-coating,<sup>15</sup> or via solution-phase self-assembly.<sup>16</sup> Here we use the *zone-casting method*<sup>17</sup> to deposit aligned thin films of PEN from solution onto various gate dielectric substrates that have not been preoriented.

The zone-casting method has been used previously by Tracz et al.<sup>18</sup> and Pisula et al.<sup>19,20</sup> for the alignment of discotic liquid crystals of hexa-*peri*-hexabenzocoronenes (HBCs) and by Tang et al.<sup>21</sup> for the long-range ordering of block-copolymers made of polyacrylonitrile and poly(*n*-butyl acrylate). Miskiewicz et al.<sup>22</sup> aligned the small-molecule tetrakis-(octadecylthio)-tetrathiafulvalene (TTF-4SC18) into one-dimensional stacks with an average field-effect mobility of 0.01 cm<sup>2</sup>/(V s). The same group also reported the alignment of rubrene<sup>23</sup> by zone-casting onto an oxidized silicon substrate, with a field-effect mobility of 0.04 cm<sup>2</sup>/(V s), which was 1 order of magnitude lower than the mobility achieved by Stingelin-Stutzmann et al.<sup>24</sup> (0.7 cm<sup>2</sup>/(V s)) by employing another solution processing method of rubrene. Here we show that, by a careful selection of the deposition conditions and of the gate dielectric materials, it is possible to fabricate zone-cast PEN devices with performance comparable or higher than reference devices made by vacuum sublimation of PEN onto identically prepared substrates (same electrode thickness, device configuration, and gate dielectric).<sup>25</sup>

## Experimental Section

**TFT Fabrication.** Transistors were prepared in bottom gate, top contact configuration onto oxidized silicon substrates (300 nm SiO<sub>2</sub>). They were cleaned in an ultrasonic bath for 15 min in de-ionized water, acetone, and iso-propanol and then oxygen plasma cleaned for 10 min using a Tegal Plasma Etcher. The dielectric layers (BCB, C-PVP, C-PMMA) were deposited as 70–100 nm thick films by spin-coating for 30–60 s at 2000 rpm inside a glovebox with inert (nitrogen) atmosphere. The pentacene was spin-cast, drop-cast, and zone-cast from a solution in an anhydrous chlorinated solvent (1–2 mg/mL) inside a nitrogen glovebox. The solution temperature was held at 160–190 °C, while the sample temperature was varied between 170–180 °C for optimized pentacene crystal growth. All solution preparation, film growth, and device preparation steps were performed in a cleanroom with yellow room lighting.

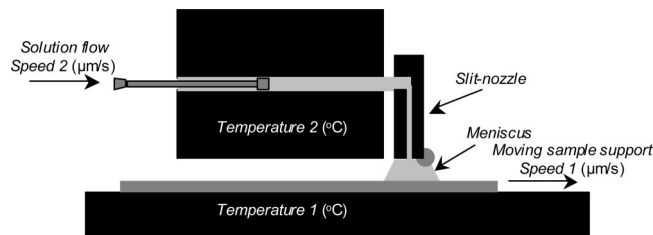


**Figure 1.** Zone-casting experimental setup. The sample temperature and speed (T1, S1) can be controlled independently from the solution temperature and supply rate (T2, S2) to give a stable meniscus.

**Microstructural Characterization.** Optical and polarized optical images were taken using an Olympus BX51 microscope, whereas the AFM characterization was performed with a Dimension 3100 system from Digital Instruments. The specular X-ray investigation was undertaken using a Bruker AXS diffractometer. The grazing incidence X-ray diffraction took place at the HASYLAB synchrotron facility using beam line BW2. The measurements were done with a wavelength of 1.240 Å and beam dimensions of 1 mm × 0.01 mm ( $h \times v$ ), and the scattered intensity was collected using a scintillation point detector.

## Results and Discussion

**Alignment of PEN Films by Zone-Casting.** Aligned layers of PEN were prepared using an in-house built zone-casting setup assembled to the specification provided by W. Pisula and K. Müllen at the Max-Planck Institute for Polymer Research, Mainz, Germany. The solution of PEN in an anhydrous chlorinated solvent (1–2 mg/mL) was continuously supplied through a stationary slit-like nozzle onto a moving substrate (Figure 1). To prevent the oxidation of the PEN solution,<sup>26</sup> the casting took place in a glovebox with inert nitrogen atmosphere (<10 ppm oxygen). The sample and solution temperatures (T1 and T2 in Figure 1) were independently controlled by two separate heater blocks, and maintained at 170–180 and 160–190 °C, respectively. To achieve a stable meniscus, two stepper motors controlled independently the motion of the sample and the solution supply rates (S1 and S2 in Figure 1). The temperature difference between nozzle and sample plate and the rates of solution supply and substrate motion were optimized to obtain stationary film solidification conditions.

The substrates used for TFT manufacturing were oxidized silicon wafers whose surface was modified either by hexamethyldisilazane (HMDS) or by spinning a thin (approximately 70 nm thick) buffer layer of a polymer dielectric. For HMDS treatments longer than 3 min the PEN solution did not wet the substrate, and consequently such films were not used for device manufacturing. The thickness of the zone-cast PEN films was approximately 100 nm, with PEN monocrystalline domains spanning several squared millimeters.

**Optical Microscopy of Solution-Cast PEN Films.** Figure 2 shows optical micrographs (same scale bar, μm) of PEN films deposited from solution by employing three different deposition methods: spin-coating, drop-casting, and zone-casting. Spin-coating the PEN solution onto preheated

- (14) Lee, W. H.; Kim, D. H.; Jang, Y.; Cho, J. H.; Hwang, M.; Park, Y. D.; Kim, Y. H.; Han, J. I.; Cho, K. *Appl. Phys. Lett.* **2007**, *90*, 132106.
- (15) Headrick, R. L.; Zhou, H.; Ruiz, R.; Mayer, A. C.; Malliaras, G. G.; Kazimirov, A. *Powder Diffraction* **2004**, *19*, 205.
- (16) Kim, D. H.; Lee, D. Y.; Lee, H. S.; Lee, W. H.; Kim, Y. H.; Han, J. I.; Cho, K. *Adv. Mater.* **2007**, *19*, 678.
- (17) Tracz, A.; Pakula, T.; Jeszka, J. K. *Mater. Sci. (Pol.)* **2004**, *22*, 415.
- (18) Tracz, A.; Jeszka, J. K.; Watson, M. D.; Pisula, W.; Müllen, K.; Pakula, T. *J. Am. Chem. Soc.* **2003**, *125*, 1682.
- (19) Pisula, W.; Tomović, Z.; Stepputat, M.; Kolb, U.; Pakula, T.; Müllen, K. *Chem. Mater.* **2005**, *17*, 2641.
- (20) Pisula, W.; Menon, A.; Stepputat, M.; Lieberwirth, I.; Kolb, U.; Tracz, A.; Siringhaus, H.; Pakula, T.; Müllen, K. *Adv. Mater.* **2005**, *6*, 684.
- (21) Tang, C.; Tracz, A.; Kruk, M.; Zhang, R.; Smilgies, D.-M.; Matyjaszewski, K.; Kowalewski, T. *J. Am. Chem. Soc.* **2005**, *127*, 6918.
- (22) Miskiewicz, P.; Marszałek, T.; Jung, J.; Kotarba, S.; Glowacki, I.; Gomar-Nadal, E.; Amabilino, D. B.; Veciana, J.; Krause, B.; Carbone, D.; Rovira, C.; Ulanski, J. *Chem. Mater.* **2006**, *18*, 4724.
- (23) Miskiewicz, P.; Marszałek, T.; Jung, J.; Kotarba, S.; Maniukiewicz, W.; Ulanski, J. Presented at ICOE, 2007; Abstract 35.
- (24) Stutzmann-Stingelin, N.; Smits, E.; Wondergem, H.; Tanase, C.; Blom, P.; Smith, P.; de Leeuw, D. *Nat. Mater.* **2005**, *4*, 601.
- (25) Duffy, C. M.; Tello, M.; Chiesa, M.; Siringhaus, H.; Ando, M.; Minakata, T.; Andreasen, J. W.; Breiby, D. W. Presented at ECME, 2007; Contributed Talk CO-8.

- (26) Maliakal, A.; Raghavachari, K.; Katz, H.; Chandross, E.; Siegrist, T. *Chem. Mater.* **2004**, *16*, 4980.



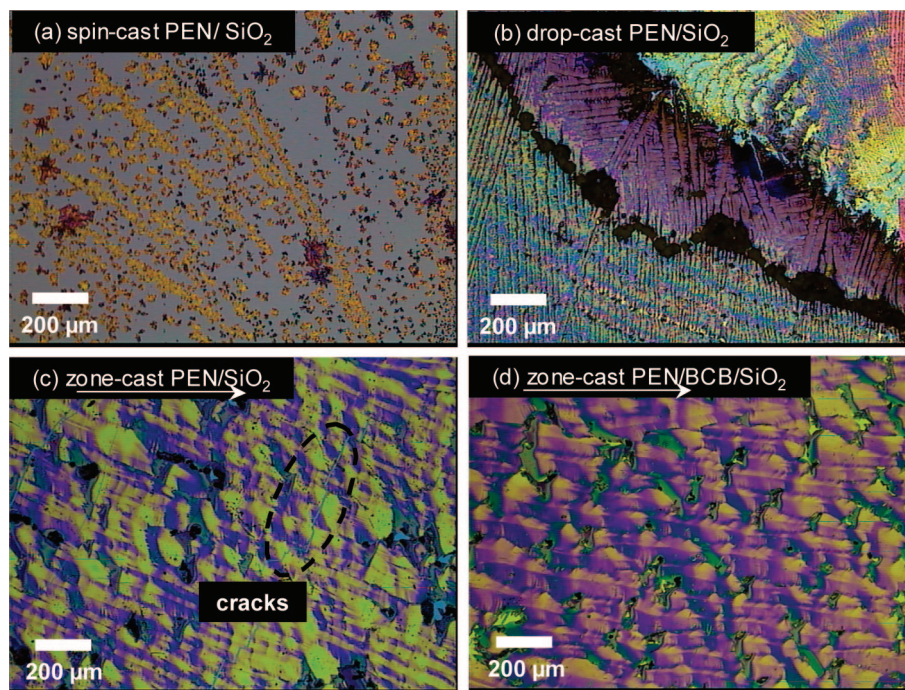


**Figure 2.** Improvement of the PEN alignment by choosing a suitable casting method: (a) dispersed crystals by spin-coating, (b) aligned domains between contact lines by drop-casting, and (c, d) directional alignment by zone-casting (the arrows indicate the zone-casting direction, from left to right in these images).

samples generally led to uncontrolled crystallization with small and dispersed crystals (brown-yellow crystalline aggregates in Figure 2a), with a radial distribution induced by the shear forces acting during spinning. The poor film quality is an indication that spin-coating is not a suitable deposition technique for low-viscosity solutions of unsubstituted pentacene molecules. The drop-casting method was a more controlled deposition, which led to aligned films of PEN. However, the long-range order in the films (Figure 2b) was disrupted by the presence of many contact lines, which are created by the receding motion and frequent pinning of the liquid contact line during the solidification process. The elongated grain orientation was disrupted by each of these contact lines. The best long-range film alignment (Figure 2c,d) was obtained by using the zone-casting technique, which proved to be a controllable and reproducible deposition method. Stationary film growth conditions and avoidance of contact lines were achieved by carefully selecting the solution supply rate, sample velocity, and substrate/solution temperatures. The morphology of the zone-cast films, as observed from the optical micrographs, is characterized by elongated crystalline grains, which are typically 10–100  $\mu\text{m}$  wide and extend for several millimeters along the zone-casting direction. The long axis of these grains is preferentially aligned along the zone-casting direction, with some domains making discrete orientation deviations of up to 35° to the zone-casting direction (see discussion of in-plane orientation below). The film shown in Figure 2c was deposited onto an unmodified SiO<sub>2</sub>/Si substrate. The crystalline alignment was disrupted by deep cracks, usually arranged perpendicular to the axis of the elongated crystalline grains. The cracks appeared soon after the film was formed and were most likely caused by the difference between the thermal expansion coefficients of PEN and SiO<sub>2</sub>. We found that the

presence of a soft, polymeric buffer layer between the PEN film and the SiO<sub>2</sub> prevented the appearance of such cracks. The choice of polymer for such a buffer layer was critical to the film formation because the polymer had to successfully withstand the high casting temperatures and chlorinated solvent exposure during TFT manufacturing. BCB (divinylsiloxane-bis-benzocyclobutene resin) and C-PVP (cross-linked poly(vinyl-phenol)) allowed the formation of uniform films, whereas the C-PMMA (cross-linked poly(methyl-methacrylate)) dissolved upon solvent application, leading to nonuniform films.

**AFM Investigation of Zone-Cast PEN Films.** Atomic force microscopy (AFM) was used to investigate the film morphology in more detail (Figure 3). PEN films deposited onto SiO<sub>2</sub>/Si and BCB modified SiO<sub>2</sub>/Si (Figure 3a,b) exhibited highly crystalline elongated grains aligned close to the zone-casting direction (from left to right in Figure 3a,b). Along the zone-casting direction the elongated grains were extremely smooth with wide, flat terraces (typical roughness rms = 0.3 nm). Perpendicular to the casting direction the film was terraced, with significant thickness variations. Step heights of approximately 1.4–1.5 nm were measured, corresponding to the length of a single PEN molecule corrected by a tilt angle with respect to the substrate. Figure 3a shows how the cracks in the films cast on SiO<sub>2</sub>/Si disrupted the crystalline order by creating deep trenches and therefore interrupting the path for charge transport (see discussion below). Figure 3c illustrates the problems that arose when buffer layers were used that did not have sufficient solvent resistance. The rough film depicted in Figure 3c was cast onto C-PMMA/SiO<sub>2</sub>/Si and did not display the typical terraced structure of the other PEN films.

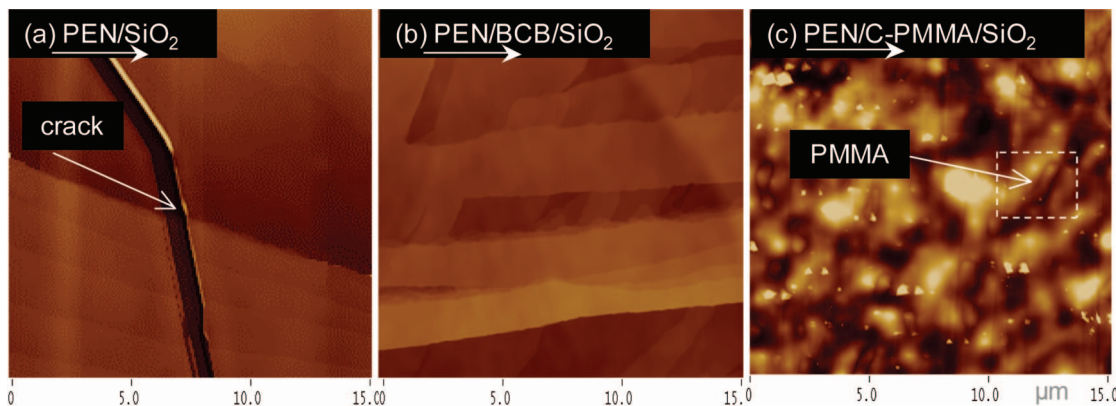


**Figure 3.** AFM images of zone-cast PEN films: (a) on unmodified SiO<sub>2</sub>, showing the presence of deep cracks; (b) highly aligned domains on BCB/SiO<sub>2</sub>; and (c) on C-PMMA/SiO<sub>2</sub> with PMMA regions incorporated in the PEN crystalline matrix (marked area). The arrows indicate the zone-casting direction, from left to right in these images (the AFM height scale is 50 nm).

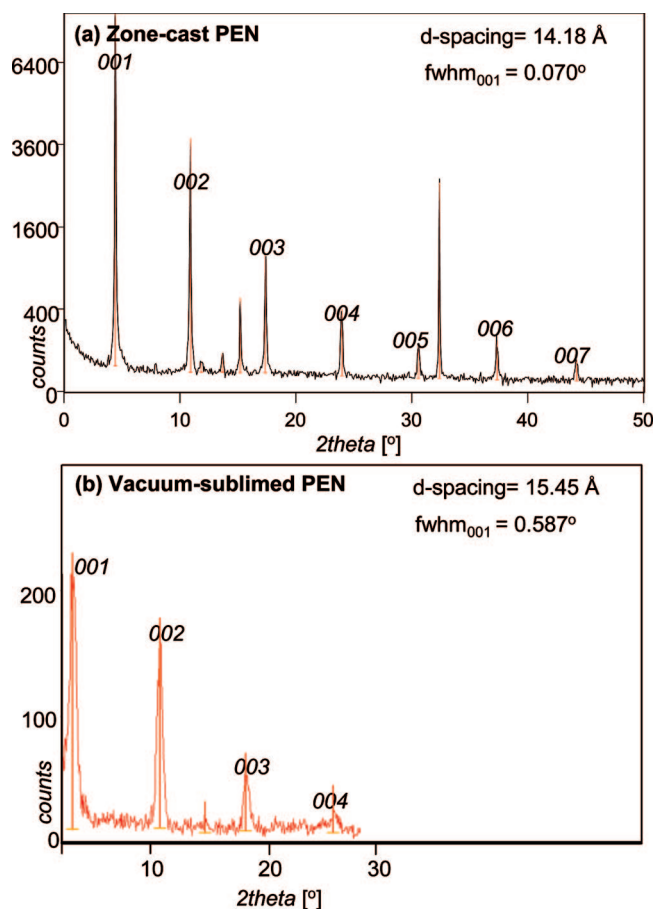


**Figure 4.** Specular X-ray scans of (a) 100 nm zone-cast PEN on unmodified SiO<sub>2</sub> and (b) of 50 nm vacuum-sublimed PEN films on HMDS treated SiO<sub>2</sub>.

The marked area in Figure 3c provides an insight into the structure of the rough film surface by revealing amorphous-looking inclusions that might be PMMA domains incorporated into the PEN crystalline matrix. The rough morphology was caused by the C-PMMA dissolving upon the application of the hot PEN solution.

**Molecular Structure of Aligned PEN Films.** The crystalline structure of the PEN films zone-cast on oxidized silicon substrates was also investigated by *symmetric*  $\Theta$ - $2\Theta$  *specular* X-ray diffraction (Figure 4), performed using Cu K $\alpha$  radiation (wavelength 1.5418 Å). The X-ray measure-

ment of the zone-cast film on SiO<sub>2</sub>/Si showed the 001 reflection at 6.23° and its higher order 00*n* up to at least *n* = 7, corresponding to a *d*-spacing of 14.18 Å (Figure 4a). The molecular packing of the zone-cast films was compared with the structure of the vacuum sublimed PEN films. Killampali et al.<sup>27</sup> and Shtein et al.<sup>28</sup> reported an improvement of the evaporated PEN thin-film morphology by modifying the surface of the SiO<sub>2</sub> with self-assembled monolayers of hexamethyldisilazane (HMDS) and octadecyltrichlorosilane (OTS), respectively. Therefore, to improve the grain size of the vacuum-sublimed reference samples, we evaporated PEN onto SiO<sub>2</sub> treated with HMDS. The films revealed a pronounced terraced structure with grain widths of hundreds of nanometers (AFM image not shown here). However, the X-ray diffractogram of the evaporated film displayed fewer and less intense peaks compared to the zone-cast film. The 001 reflection was identified at 5.72°, with higher order 00*n* up to *n* = 4, corresponding to a *d*-spacing of 15.45 Å (Figure 4b). The interplanar distances of 14.18 Å and 15.45 Å are in agreement with the step heights observed by AFM and corroborate the arrangement of the PEN molecules with their long axis (*c*-axis of the triclinic unit cell) tilted with respect to the substrate surface, making an angle with the surface normal of 29° for the zone cast films and 17° for the vacuum sublimed PEN. Mattheus et al.<sup>29,30</sup> synthesized four different polymorphs of PEN, which could be identified by their layer periodicity as the 14.12, 14.4, 15.0, and 15.4 Å polymorphs. Bulk single crystals commonly adopted the 14.12 Å structure, whereas all other three polymorphs could be synthesized in thin-film form depending on the growth conditions. The 00*l* spacing of 14.18 Å of our zone-cast PEN films suggests a molecular packing very close to that of the *bulk-phase* of PEN as determined by Campbell et al.,<sup>31</sup> whereas the spacing of 15.45 Å of the vacuum-sublimed films is characteristic of the *thin-film phase* of PEN.<sup>30</sup> The presence of many higher

(27) Killampali, A. S.; Engstrom, J. R. *Appl. Phys. Lett.* **2006**, *88*, 143125.

(28) Shtein, M.; Mapel, J.; Benziger, J. B.; Forrest, S. R. *Appl. Phys. Lett.* **2002**, *81*, 268.

(29) Mattheus, C. C.; Dros, A. B.; Baas, J.; Oostergetel, G. T.; Meetsma, A.; de Boer, J. L.; Palstra, T. M. *Synth. Met.* **2003**, *138*, 475.

(30) Mattheus, C. C.; Dros, A. B.; Baas, J.; Meetsma, A.; de Boer, J. L.; Palstra, T. M. *Acta Crystallogr., Sect. C* **2001**, *C57*, 939.

(31) Campbell, R. B.; Robertson, J. M. *Acta Crystallogr.* **1962**, *15*, 289.



order reflections and the narrower peak widths of the zone-cast PEN diffractogram ( $\text{fwhm}_{001} = 0.070^\circ$  compared to  $\text{fwhm}_{001} = 0.587^\circ$  of the vacuum-sublimed films) indicate a high degree of long-range order of the intermolecular layered stacking of the PEN molecules along the substrate normal. The diffractograms in Figure 4 displayed additional reflections at  $15.10^\circ$ ,  $16.56^\circ$ , and  $33.03^\circ$ . They are tentatively identified as reflections from PEN crystals, possibly different polymorphs, with a random orientation in the film.

The samples were measured by grazing incidence X-ray diffraction (GIXD) to characterize the in-plane (i.e., the surface plane) texture of the zone-cast PEN crystallites. This method has been employed previously by Breiby et al. for investigating the crystalline structure<sup>32</sup> and the effect of the crystalline to liquid crystalline phase transition on the molecular packing<sup>33</sup> of zone-cast HBC- $\text{C}_{12}\text{H}_{25}$  films. On the basis of our previous findings, the zone-cast PEN films adopt the bulk-phase structure, and therefore we used the triclinic unit cell parameters defined by Campbell ( $a = 7.9 \text{ \AA}$ ,  $b = 6.06 \text{ \AA}$ ,  $c = 16.01 \text{ \AA}$ ,  $\alpha = 101.9^\circ$ ,  $\beta = 112.6^\circ$ ,  $\gamma = 85.8^\circ$ ) for the GIXD data analysis. For GIXD measurements the sample surface normal was parallel to the phi-rotation axis of the diffractometer, and the sample surface was inclined with respect to the incoming beam by  $0.16^\circ$ . At this shallow angle, the beam is totally reflected from the oxidized silicon substrate surface and only the zone-cast PEN film contributes to the diffracted signal. The GIXD measurements are consistent with the pentacene unit cells being oriented with the  $ab$ -plane parallel to the substrate. The in-plane texture was determined from the  $\varphi$  rocking scans by setting the point detector at a position corresponding to an in-plane PEN reflection and "rocking" the sample through different angles around the surface normal. The angle  $\varphi = 0$  corresponds to the incoming X-ray wavevector being perpendicular to the zone-casting direction. The  $\varphi$ -scan at the  $\bar{2}11$  reflection, shown in Figure 5a, exhibits relatively few and very sharp peaks. This provides clear evidence for the pronounced in-plane alignment of the large PEN domains in contrast to vacuum-sublimed polycrystalline films with no in-plane anisotropy. Because the individual crystalline domains are very large, we have observed some dependence of the rocking scans on the exact location of the incident beam on the sample. However, two peak pairs are consistently observed in the zone-cast samples, each with  $180^\circ$  symmetry, that is, the reflections at  $[-47^\circ, 133^\circ (= -47^\circ + 180^\circ)]$  and  $[24^\circ, -156^\circ (= 24^\circ - 180^\circ)]$ . The few very sharp and intense peaks in the rocking scan (Figure 5a) are attributed to the large monocrystalline domains observed under crossed-polarizers in the polarized optical micrographs shown as an inset of Figure 7. A  $180^\circ$  symmetry in  $\varphi$  is expected for in-plane reflections having  $\mathbf{Q}$  nearly parallel to the substrate plane, which holds for both  $\bar{2}11$  and  $\bar{1}10$  reflections of the triclinic cell studied here (for out-of-plane reflections, the Friedel symmetry related peaks would appear below the substrate horizon). The presence of two peak pairs

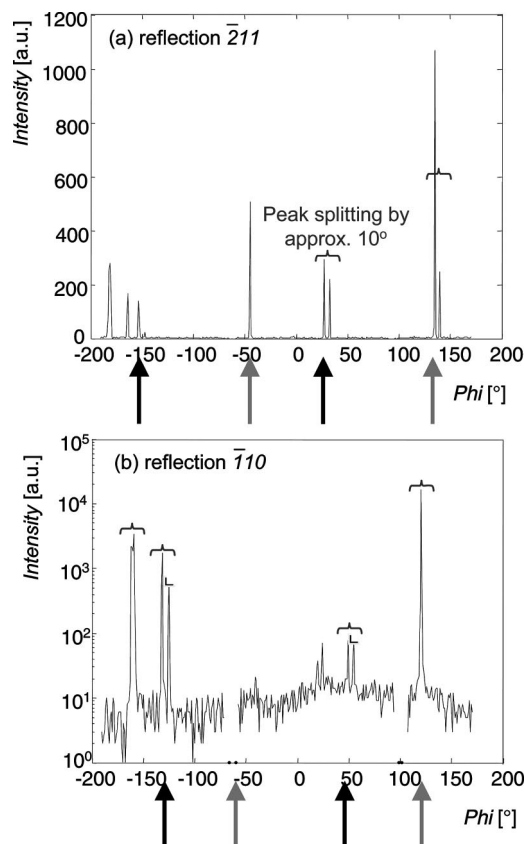


**Figure 5.** Phi scans at the (a)  $\bar{2}11$  and (b)  $\bar{1}10$  reflections of the zone-cast PEN on  $\text{BCB}/\text{SiO}_2$  showing very few and sharp peaks with a  $180^\circ$  symmetry. The peak splitting by approximately  $10^\circ$  is an indication of twin-related crystalline domains sharing the same  $a$ -axis (refer to illustration in Figure 6).

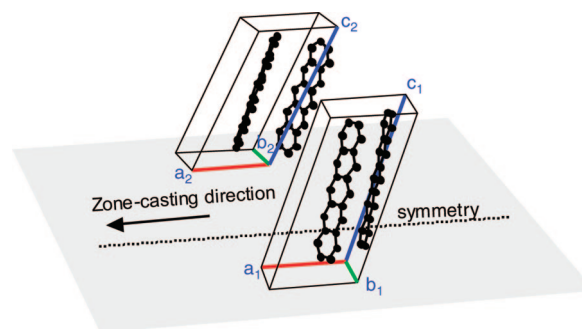


**Figure 6.** Illustration of the PEN triclinic unit cell showing two energetically equivalent twin-related domains (unit cell 1 and unit cell 2), with the same  $a$ -axis orientation parallel to the zone-casting direction.

corresponds to equivalent grains with the  $a$ -axis parallel to the zone-casting direction but rotated by  $180^\circ$  around the  $a$ -axis/zone-casting direction (see illustration in Figure 6), that is, *twinning*. For this particular situation, the twin law (defined by Hahn and Klapper<sup>34</sup> in the *International Tables for Crystallography*) describes the twins related by twofold rotation around the common  $100$  direction, here designated as the  $100$  twofold twin axis. Rocking scans at the  $\bar{1}10$  reflection (shown in Figure 5b) corroborate the results for the  $\bar{2}11$  reflection, that is, with two groups of reflections at

(32) Breiby, D. W.; Bunk, O.; Pisula, W.; Sølling, T. I.; Tracz, A.; Pakula, T.; Müllen, K.; Nielsen, M. M. *J. Am. Chem. Soc.* **2005**, *127*, 11288.  
 (33) Breiby, D. W.; Hansteen, F.; Pisula, W.; Bunk, O.; Kolb, U.; Andreasen, J. W.; Müllen, K.; Nielsen, M. M. *J. Phys. Chem. B* **2005**, *109*, 22319.

(34) Hahn, T.; Klapper, H. *International Tables for Crystallography*; International Union of Crystallography: Chester, U.K., 2006; Vol. D, Chapter 3.3, pp 393–448.

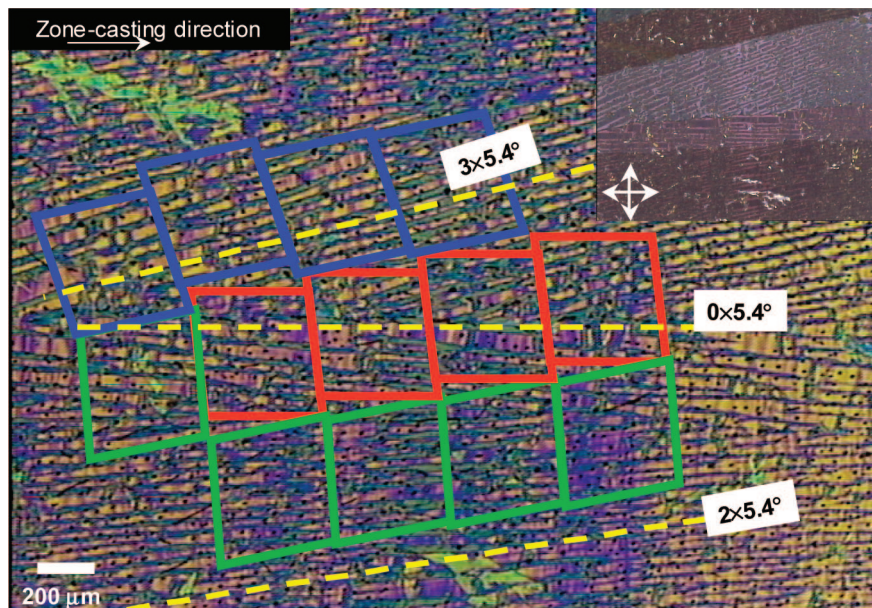


**Figure 7.** Optical micrograph and the corresponding polarized optical image (inset) of the zone-cast PEN film showing that the predominant orientation of the monocrystalline domains is either parallel to the zone-casting direction or making an angle of multiples of  $5.4^\circ$  with the majority orientation. The parallelograms indicate the orientation of the  $ab$  facet of the triclinic unit cell<sup>31</sup> with respect to the substrate (not to scale).

$(-61^\circ, 119^\circ)$  and  $(46^\circ, -134^\circ)$  having  $180^\circ$  symmetry. Note that the experimental setup shadowed the symmetrical partner of the strongest peak at  $119^\circ$ , thus leading to missing points at  $-70^\circ$  and  $-60^\circ$  in Figure 5b.

Depending on the sample position, we observed other well defined domain orientations, for which the  $a$ -axis is oriented at angles of small multiples of  $5.4^\circ$  from the zone-casting direction. The overall orientation of the crystalline domain is determined by the orientation of the crystal's facet for which the growth rate is the highest and crystals of significantly different orientations with respect to the zone-casting direction will grow significantly slower as the casting proceeds. Northrup et al.<sup>35</sup> studied the PEN growth at higher substrate temperatures and suggested that some degree of transport could occur between different step facets, and so the growth velocity of steps is expected to be orientation dependent. Our results suggest that, under the growth conditions employed during zone-casting, the growth is fastest along the  $a$ -axis of the unit cell, and that well defined, low-energy domain boundaries exist that lead to minority domain orientations making an angle of multiples of  $5.4^\circ$  with the majority orientation ( $a$ -axis along the zone-casting direction). Note that  $5.4^\circ$  ( $90^\circ - \gamma$ ) is close to the angle  $\gamma = 86.4^\circ$  between the normal to the  $a$ -axis and the  $b$ -axis. From the rocking curve data (Figure 5a,b) it can be seen that several peaks exhibit a splitting by approximately  $10^\circ$  ( $= 2 \times 5.4^\circ$ ), agreeing with the deviation of  $\gamma$  from  $90^\circ$ . A certain possibility exists for finding crystallites differing from the dominant orientation (the  $a$ -axis) by  $n \times 5.4^\circ$  ( $n$  is a small integer), suggesting another twin law with an operation element parallel to some low index lattice orientation or plane (not identified). Figure 7 illustrates this tentative  $n \times 5.4^\circ$  twin-growth model by showing the large monocrystalline

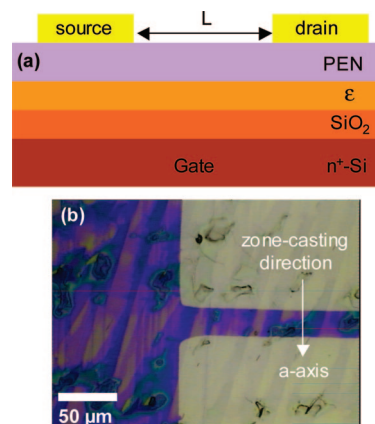


**Figure 8.** (a) Cross-sectional view and (b) optical micrograph of a bottom-gate, top-contact PEN device with the channel arranged parallel to the zone-casting direction ( $L = 20 \mu\text{m}$ ,  $W = 1000 \mu\text{m}$ ) ( $\epsilon$  = BCB, C-PVP, C-PMMA).

domains under cross-polarizers and indicating their preferred growth orientations with respect to the zone-casting direction.

**Charge Transport Anisotropy.** TFTs were fabricated in a standard bottom-gate, top-contact configuration (Figure 8a). The oxidized silicon substrates were cleaned by acetone, isopropanol, and oxygen plasma etch. Either they were used as-cleaned ( $\text{SiO}_2$  interface), or a buffer polymer dielectric layer (labeled  $\epsilon$  in Figure 8a) was spun as a 70–100 nm thin film. Here we used BCB, C-PVP, and C-PMMA. Then, the PEN was zone-cast according to the optimized conditions presented earlier, followed by a 30 nm Au deposition through shadow masks, leading to channel lengths of 425, 275, and  $20 \mu\text{m}$ . A typical optical micrograph of the  $20 \mu\text{m}$  channel was used in Figure 8b to illustrate the geometry of the electrodes and the high quality of the PEN film present in the transistor's channel. The TFT characteristics were measured in a glovebox with an inert nitrogen atmosphere (2–3 ppm oxygen), using an Agilent 4155B semiconductor parameter analyzer. We measured the transfer curves for all

(35) Northrup, J. E.; Tiago, M. L.; Louie, S. G. *Phys. Rev. B* **2002**, *66*, 121404.



devices by sweeping the gate voltage  $V_g$  from 0 to  $-60$  V and keeping the drain bias  $V_d$  at either  $-5$  V (linear regime) or  $-60$  V (saturation regime). The charge carrier mobility,  $\mu$ , was derived from the transfer curves in the saturation regime by using the equation  $I_{d,sat} = (W/2L)\mu C_i (V_g - V_{th})^2$ , where  $L$  and  $W$  are the channel length and width, respectively,  $C_i$  is the total capacitance of the insulator per unit area (11.51 nF/cm<sup>2</sup> for SiO<sub>2</sub>, 7.85 nF/cm<sup>2</sup> for BCB/SiO<sub>2</sub>, 9.63 nF/cm<sup>2</sup> for C-PVP/SiO<sub>2</sub>, and 7.86 nF/cm<sup>2</sup> for C-PMMA/SiO<sub>2</sub>, as calculated from measured dielectric thickness), and  $V_{th}$  is the threshold voltage obtained from the intercept with the  $x$ -axis of the linear fit of the plot  $\sqrt{I_{d,sat}}$  versus  $V_g$ . Generally, TFT performance was reproducible and high field-effect mobilities up to 0.4–0.7 cm<sup>2</sup>/(V s) were obtained.

The GIXD data reveals a pronounced in-plane anisotropy of the PEN crystalline domains, with the  $ab$ -plane parallel to the substrate and the  $a$ -axis oriented mainly parallel to the zone-casting direction. We also investigated the anisotropy in the charge transport by preparing bottom-gate, top contact TFTs with the channel arranged either parallel or perpendicular to the zone-casting direction, that is, the charge transport occurs either along the  $a$ -axis or the  $b$ -axis of the unit cell. Polarized optical microscopy was used first to identify large monocrystalline domains having the same predominant molecular orientation with respect to the zone-casting direction for PEN films deposited onto the BCB/SiO<sub>2</sub> substrate. Then, we evaporated Au source-drain electrodes (30nm) through shadow masks selectively placed over these monocrystalline regions. The resulting devices had a channel length of 20  $\mu$ m and a width of 1000  $\mu$ m. Owing to the large size of the PEN crystals it was easy to place the transistor's channel such as to avoid any film imperfections and to ideally cover one or two monocrystalline domains. The Si substrate was used as the transistor's gate, and the resulting device characteristics are shown in Figure 9a,b, where the red curves are associated with transistor channels perpendicular to the zone-casting direction and the blue curves with channels parallel to the casting direction. From the transfer characteristics (Figure 9a) we calculated the threshold voltage,  $V_{th}$ , and the mobility,  $\mu_{sat}$ , of the two types of devices (the charge carrier mobility was calculated from the saturation regime of each transfer curve). For the TFT with the channel perpendicular to the casting direction, that is, charge transport preferentially along the  $b$ -axis of the unit cell, the threshold voltage was  $-17.2$  V with a mobility of 0.308 cm<sup>2</sup>/(V s), whereas the device whose channel was parallel to the casting direction, that is, charge transport preferentially along the  $a$ -axis of the unit cell, had a threshold voltage of  $-17.8$  V and a mobility of 0.204 cm<sup>2</sup>/(V s) (see optical image in Figure 8b). The on-off ratios of the two devices were similar (approximately 10<sup>6</sup>). The output curves at small source-drain voltages in Figure 9b show that contact resistance effects between the Au electrodes and the PEN crystals do not limit the device performance in either of the two device configurations. The observed charge transport anisotropy of  $\mu_b/\mu_a = 1.5$  is smaller compared to that measured for rubrene single crystals (mobility anisotropy =

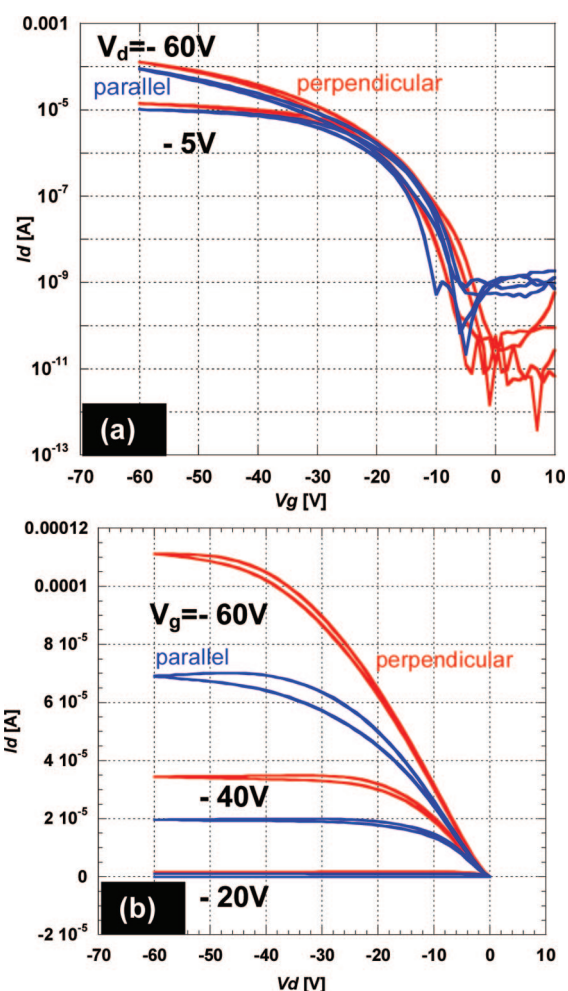


**Figure 9.** (a) Transfer and (b) output characteristics of two 20  $\mu$ m  $\times$  1000  $\mu$ m PEN devices zone-cast on BCB/SiO<sub>2</sub> where the channel was placed either perpendicular (red curves) or parallel (blue curves) to the zone-casting direction.

2.7)<sup>36</sup> or for PEN single crystals (mobility anisotropy = 3.5).<sup>37</sup> It is tempting to interpret this small anisotropy of charge transport in terms of the high degree of crystalline order present in the packing direction (edge-to-face),<sup>38</sup> making it equally possible for the charges to be transported either along the  $a$ -axis or the  $b$ -axis. To further confirm this small charge transport anisotropy we inverted the source and drain contacts of a TFT deposited onto BCB/SiO<sub>2</sub> and having the channel parallel to the zone-casting direction and measured the drain currents  $I_d$  (electrical characteristics not shown). The magnitude of the drain currents was similar for both configurations, indicating that the triclinic unit cell of PEN does not show any asymmetry to charge transport and suggesting excellent inversion symmetry of the crystalline structure. These results are consistent with the findings of Lee et al.<sup>37</sup> on single crystals of PEN grown by the horizontal physical vapor deposition method. However, it cannot be excluded that, in the present device, grain boundaries and morphological effects, such as the significant thickness variations perpendicular to the zone-casting direction, may also affect the measured anisotropy.

(36) Reese, C.; Bao, Z. *Adv. Mater.* **2007**, *19*, 4535.

(37) Lee, J. Y.; Roth, S.; Park, Y. W. *Appl. Phys. Lett.* **2006**, *88*, 252106.

(38) Troisi, A.; Orlandi, G. *J. Phys. Chem. B* **2005**, *109*, 1849.

**Table 1. Saturation Mobilities of PEN TFTs Made by Zone-Casting<sup>a</sup>**

	425 $\mu\text{m}$	$\mu_{\text{sat}}$ ( $\text{cm}^2/(\text{V s})$ )	
		275 $\mu\text{m}$	20 $\mu\text{m}$
SiO <sub>2</sub>	0.050	0.030	0.187
BCB/SiO <sub>2</sub>	0.154	0.181	0.308
C-PVP/SiO <sub>2</sub>	0.061	0.066	0.080
C-PMMA/SiO <sub>2</sub>	poor	poor	0.050

<sup>a</sup> Mobility increases when the channel length is decreased from 425  $\mu\text{m}$  to 20  $\mu\text{m}$ , with the highest mobility for BCB/SiO<sub>2</sub> (best crystalline alignment) (all TFT channels were aligned parallel to the zone-casting direction).

**Influence of Dielectric on TFT Performance.** The film morphology and consequently the device performance of the zone-cast PEN devices were found to depend significantly on the surface properties of the underlying gate dielectric layer. Table 1 summarizes the mobility values as a function of the channel length obtained for devices with channels aligned parallel to the zone-casting direction. In the case of the SiO<sub>2</sub> gate dielectric the mobility in the long channel devices ( $L = 425 \mu\text{m}$ ,  $275 \mu\text{m}$ ) is 1 order of magnitude lower than that of short channel devices ( $L = 20 \mu\text{m}$ ). This is attributed to the presence of cracks perpendicular to the elongated grains. These occur typically on a length scale of several 100  $\mu\text{m}$  and, by reducing the channel length, we avoid the incorporation of such cracks into the active device area. TFTs zone-cast on BCB/SiO<sub>2</sub> exhibited a much smaller increase in mobility with decreasing channel length, thus reflecting a more uniform morphology. Generally BCB was the most suitable gate dielectric, yielding the most uniform and reproducible zone-cast films and the highest device performance. Preliminary experimental data showed that zone-cast PEN devices on BCB also exhibit excellent bias-stress stability. Device performance with C-PVP and C-PMMA was much poorer, most probably due to partial dissolution/swelling of the polymer dielectric by the hot chlorinated solvent.

## Conclusions

In this work we demonstrated high performance PEN thin-film transistors based on well-aligned PEN films made by zone-casting onto various dielectric materials, without the need for preorientation of the underlying dielectric layer. X-ray diffraction showed that the PEN film is highly crystalline and adopts a crystal structure close to that of the *bulk phase* of PEN. The crystallites are oriented with the *ab*-plane parallel to the sample substrate, and the films exhibit a pronounced in-plane anisotropy with the *a*-axis of the unit cell aligned preferentially close to the zone-casting direction. The surface of the substrate is critical to achieving uniform and reproducible film morphology, and BCB was found to be a suitable buffer gate dielectric layer. Field-effect mobilities of 0.4–0.7  $\text{cm}^2/(\text{V s})$  were reproducibly obtained, which are comparable or better than those of reference PEN devices fabricated by vacuum sublimation. *Zone-casting* is a powerful technique for the solution deposition of aligned films of small-molecule organic semiconductors.

**Acknowledgment.** This work was funded by Hitachi and the Cambridge European Trust. M.M.N. and D.W.B. would like to acknowledge the financial support from the Danish National Research Foundation. We also acknowledge HASYLAB for providing synchrotron beam time and DANSYNC for funding the synchrotron experiments. The pentacene solution was supplied by Asahi Kasei Corporation. The cross-linked PMMA and PVP films (C-PMMA and C-PVP) were prepared in collaboration with Dr. Y. Y. Noh, Cambridge University. We are delighted to acknowledge the collaboration with Dr. W. Pisula and Prof. K. Müllen from the Max Planck Institute for Polymer Research in Mainz, Germany, which enabled us to setup the zone-casting experimental system.

CM801689F